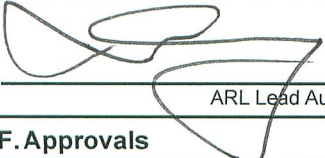
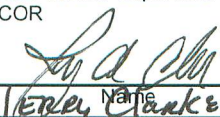
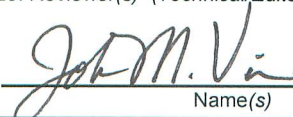


3374

Quality Assurance and OPSEC Review

2874

This form is an approval record for ARL generated information to be presented or disseminated external to ARL. Note: Submit all manuscripts in electronic format or camera ready copy. See attached instructions. If more space is needed, use reverse of form (*include block numbers*).

A. General Information		1. Present Date 09/11/2008		2. Unclassified Title Simulations of Quantum Dot Growth on Semiconductor Surfaces:	
3. Author(s) Peter W. Chung, Ernie Pan, Melissa Sun, Richard Zhu		4. Office Symbol(s) AMSRD-ARL-CI-HC		5. Telephone Nr(s) 410278-6027	
6. Contractor generated <input type="checkbox"/> No <input type="checkbox"/> Yes If yes, enter Contract No. and ARL COR		7. Type: <input type="checkbox"/> Report <input type="checkbox"/> Abstract <input checked="" type="checkbox"/> Publication <input type="checkbox"/> Presentation (<i>speech, briefing, video clip, poster, etc</i>) <input type="checkbox"/> Book <input type="checkbox"/> Book Chapter <input type="checkbox"/> Web			
		8. Key Words Quantum Dots, nanotechnology, modeling, kinetic Monte Carlo			
9. Distribution Statement (<i>required</i>) Is manuscript subject to export control? <input checked="" type="checkbox"/> No <input type="checkbox"/> Yes		Circle appropriate letter and number. (<i>see instructions for statement text</i>) <input checked="" type="checkbox"/> B <input type="checkbox"/> C <input type="checkbox"/> D <input type="checkbox"/> E <input type="checkbox"/> F <input type="checkbox"/> X 1 2 3 4 5 6 7 8 9 10 11			10. Security Classification
B. Reports	11. Series	12. Type	13. No. of pages	14. Project No.	15. Period Covered
					16. Sponsor
C. Publications					
17. Is MS an invited paper? <input checked="" type="checkbox"/> No <input type="checkbox"/> Yes		19. Material will be submitted for publication in			
18. Publication is a refereed journal? <input checked="" type="checkbox"/> No <input type="checkbox"/> Yes		Army Science Conference Proceedings		USA	
		Journal		Country	
D. Presentations		20. Conference Name/Location Army Science Conference		21. Sponsor US Army	
22. Conference Date 12/01/2008	23. Due Date 09/22/2008	24. Conference is <input checked="" type="checkbox"/> Open to general public <input type="checkbox"/> Unclassified/controlled access <input type="checkbox"/> Classified			
25. For nonpublic meetings: Will foreign nationals be attending? <input type="checkbox"/> No <input type="checkbox"/> Yes (<i>If yes, list countries and identify International Agreement(s)</i>) <input checked="" type="checkbox"/> Don't know		26. Material will be <input type="checkbox"/> Oral presented only <input checked="" type="checkbox"/> Oral presented and published in Army Science Conference Proceedings (<i>If published, complete block 18 and 19, Section C.</i>)			
E. Authors Statement: 27. All authors have concurred in the technical content and the sequence of authors. All authors have made a substantial contribution to the manuscript and all authors who have made a substantial contribution are identified in Block 3.					
 ARL Lead Author or COR				9/11/08 Date	
F. Approvals					
28. First line Supervisor of Senior ARL Author or COR  Name: JERRY CLARKE (A) Chief CSEB		29. Reviewer(s) (<i>Technical/Editorial/NA</i>)  Name(s): Date:			
30. Limited distribution information for release to foreign nationals		31. Classified Information Classified by _____ Declassified on _____			
Foreign Disclosure _____ Date _____		Command Security Manager _____ Date _____			

OPSEC REVIEW CHECKLIST

OPSEC POC: Complete and explain any positive responses in block 9.
Note: ARL must be the proponent of the proposed information for release.

- | | |
|--|---|
| <p>1. Does this material contain Sensitive Information? <input type="checkbox"/> YES <input checked="" type="checkbox"/> NO</p> <p>2. Does this information contain state-of-the-art, breakthrough technology? <input type="checkbox"/> YES <input checked="" type="checkbox"/> NO</p> <p>3. Does the United States hold a significant lead time in this technology? <input type="checkbox"/> YES <input checked="" type="checkbox"/> NO</p> <p>4. Does this information reveal aspects of reverse engineering? <input type="checkbox"/> YES <input checked="" type="checkbox"/> NO</p> <p>5. Does this material reveal any security practices or procedures? <input type="checkbox"/> YES <input checked="" type="checkbox"/> NO</p> <p>6. Does this information reveal any security practices or procedures? <input type="checkbox"/> YES <input checked="" type="checkbox"/> NO</p> <p>7. Would release of this information be of economic benefit to a foreign entity, adversary, or allow for the development of countermeasures to the system or technology? <input type="checkbox"/> YES <input checked="" type="checkbox"/> NO</p> | <p>8. Does this material contain:</p> <p>a. Any contract proposals, bids, and/or proprietary information? <input type="checkbox"/> YES <input checked="" type="checkbox"/> NO</p> <p>b. Any information on inventions/patent application for which patent secrecy orders have been issued? <input type="checkbox"/> YES <input checked="" type="checkbox"/> NO</p> <p>c. Any weapon systems/component test results? <input type="checkbox"/> YES <input checked="" type="checkbox"/> NO</p> <p>d. Any ARL-originated studies or after action reports containing advice and recommendations? <input type="checkbox"/> YES <input checked="" type="checkbox"/> NO</p> <p>e. Weakness and/or vulnerability information? <input type="checkbox"/> YES <input checked="" type="checkbox"/> NO</p> <p>f. Any information on countermeasures? <input type="checkbox"/> YES <input checked="" type="checkbox"/> NO</p> <p>g. Any fielding/test schedule information? <input type="checkbox"/> YES <input checked="" type="checkbox"/> NO</p> <p>h. Any Force Protection, Homeland Defense (security) information? <input type="checkbox"/> YES <input checked="" type="checkbox"/> NO</p> <p>i. Information on subjects of potential controversy among military services or other federal agencies? <input type="checkbox"/> YES <input checked="" type="checkbox"/> NO</p> <p>j. Information on military applications in space, nuclear chemical or biological efforts: high energy laser information; particle beam technology; etc? <input type="checkbox"/> YES <input checked="" type="checkbox"/> NO</p> <p>k. Contain information with foreign policy or foreign relations implications? <input type="checkbox"/> YES <input checked="" type="checkbox"/> NO</p> |
|--|---|

OPSEC Approval Statement

I, the undersigned, am aware of the adversary's interest in DOD publications and in the subject matter of this material and that, to the best of my knowledge, the net benefit of this release outweighs the potential damage to the essential security of all ARL, AMC, Army, or other DOD programs of which I am aware.

Dale R. Shiner *Dale Shiner*
 OPSEC Reviewer (Printed name/signature)

9/16/08
 Date

9. Space for explanations/continuations/OPSEC review comments

Final Release Clearances

32. Public/Limited release information

a. Material has been reviewed for OPSEC policy.

Erich W. Meyerhoff
 ARL OPSEC Officer

9/22/08
 Date

b. The information contained in this material is ☒ / is not ☐ approved for public release/ has received appropriate tech/editorial review.

C. Pietobing *C. Pietobing, Chief ACSD*
 Division Chief

17 Sep 08
 Date

c. This information is accepted for public release.

Erich W. Meyerhoff
 Public Affairs Office

9/22/08
 Date

Report Documentation Page				Form Approved OMB No. 0704-0188	
Public reporting burden for the collection of information is estimated to average 1 hour per response, including the time for reviewing instructions, searching existing data sources, gathering and maintaining the data needed, and completing and reviewing the collection of information. Send comments regarding this burden estimate or any other aspect of this collection of information, including suggestions for reducing this burden, to Washington Headquarters Services, Directorate for Information Operations and Reports, 1215 Jefferson Davis Highway, Suite 1204, Arlington VA 22202-4302. Respondents should be aware that notwithstanding any other provision of law, no person shall be subject to a penalty for failing to comply with a collection of information if it does not display a currently valid OMB control number.					
1. REPORT DATE DEC 2008		2. REPORT TYPE N/A		3. DATES COVERED -	
4. TITLE AND SUBTITLE Simulations Of Quantum Dot Growth On Semiconductor Surfaces: Morphological Design Of Sensor Concepts				5a. CONTRACT NUMBER	
				5b. GRANT NUMBER	
				5c. PROGRAM ELEMENT NUMBER	
6. AUTHOR(S)				5d. PROJECT NUMBER	
				5e. TASK NUMBER	
				5f. WORK UNIT NUMBER	
7. PERFORMING ORGANIZATION NAME(S) AND ADDRESS(ES) U.S. Army Research Laboratory Aberdeen Proving Ground, MD 21005-5067				8. PERFORMING ORGANIZATION REPORT NUMBER	
9. SPONSORING/MONITORING AGENCY NAME(S) AND ADDRESS(ES)				10. SPONSOR/MONITOR'S ACRONYM(S)	
				11. SPONSOR/MONITOR'S REPORT NUMBER(S)	
12. DISTRIBUTION/AVAILABILITY STATEMENT Approved for public release, distribution unlimited					
13. SUPPLEMENTARY NOTES See also ADM002187. Proceedings of the Army Science Conference (26th) Held in Orlando, Florida on 1-4 December 2008, The original document contains color images.					
14. ABSTRACT					
15. SUBJECT TERMS					
16. SECURITY CLASSIFICATION OF:			17. LIMITATION OF ABSTRACT UU	18. NUMBER OF PAGES 10	19a. NAME OF RESPONSIBLE PERSON
a. REPORT unclassified	b. ABSTRACT unclassified	c. THIS PAGE unclassified			

SIMULATIONS OF QUANTUM DOT GROWTH ON SEMICONDUCTOR SURFACES: MORPHOLOGICAL DESIGN OF SENSOR CONCEPTS

Peter W. Chung
U.S. Army Research Laboratory
Aberdeen Proving Ground, MD 21005-5067

Ernie Pan, Melissa Sun, Richard Zhu
University of Akron;
Akron, OH 44325-3905

ABSTRACT

Due to quantum confinement, superlattice detectors may conceivably be tuned to detect electromagnetic signatures difficult to detect with technology available today. The challenge in creating new superlattice detectors is in the growth process where the confluence of chemistry, physics, and mechanics make control of parameters nontrivial. Furthermore, the time scales involved are often prohibitive for deterministic modeling approaches. We have developed and validated a new modeling method for probabilistic modeling of superlattice growth that spans the appropriate time scales relevant for experiments. The predictions of the models have been tested successfully against numerous independent experiments. Through a fundamentally new Green's function formulation for strain interactions among quantum dots, we present a new kinetic Monte Carlo methodology that can successfully predict pattern formation on surfaces while requiring only experimentally-viable parameters as input. The new method also can be used for engineering design of dot correlations in-plane and in-bulk to predict dot alignment in general superlattices.

INTRODUCTION

Devices such as Fourier Transform Infrared (FTIR) spectrometers can detect electromagnetic signatures related to the energies of bonds in organic molecules. These energies are often in the range of $400 - 5000 \text{ cm}^{-1}$ representing the typical absorption spectroscopy peaks for specific types of bonds. For example, the C-Br bond in bromoalkanes has an accompanying peak at 500 cm^{-1} while the O-H bond in most alcohols and phenols are around 3000 cm^{-1} . The central detector element is typically a collection of charge-coupled devices (CCD) that is each comprised of a thin semiconductor material layer whose electronic band gap energy uniquely determines the energy range of electromagnetic signal it can detect. Modern fabrication techniques involve growth of these thin layers on inexpensive substrates such as silicon. The grown layers can often be as thin as a few monolayers in height but are often no larger than a micron. At these small length scales, the interaction

between the growth and the substrate is nontrivial to the extent that the mismatch in the theoretical lattice constants can appreciably distort the overall band energy of the final system and be used as a design consideration for targeted device performance. Thus it is not uncommon to have a material grown on a substrate detect signals that the free standing material cannot.

Fabrication of these types of detector materials involves complex atomistic processes. It is now well-known that during fabrication, the interactions among the atoms in the growing layer lead to stark features on the surface known as self-assembled quantum dots (QDs). Self-assembled QDs have been intensely investigated due to observed optical and electronic properties with potential applications in a broad range of new optoelectronic and semiconductor devices (Bressler_Hill, et al., 1995; Bimberg, et al., 1998). The indium-arsenide/gallium-arsenide (InAs/GaAs) heterostructure is a typical example, which is characterized by a large lattice mismatch between alternating InAs and GaAs layers. At the growth surface, the material undergoes a transition from a two-dimensional (2D) cluster to three-dimensional (3D) islands (Stangl et al., 2004; Joyce and Vvedensky, 2004).

Experimental data indicate that InAs/GaAs island array is governed by thermodynamics (Schukin and Bimberg, 1999; Pcheljakov et al., 1997). The physics behind the transition from 2D cluster to 3D islands has been studied recently. For example, using atomic force microscopy, (Arciprete et al., 2006) studied how kinetics drives the 2D to 3D transition in InAs/GaAs(001) heterostructure. The transition from thermodynamically to kinetically controlled QD self-assembly was also studied in (Musikhin et al., 2005), both experimentally and theoretically.

It is argued that strains on the surface change diffusivity and surface mobility (Zandvliet and Poelsema, 1999; Sage et al., 2000; Zoethout et al., 2000; Pao and Srolovitz, 2006) and therefore may be the reason for the enhanced evaporation (Sun et al., 2000). The epitaxial system can lower the free energy by transferring atoms from the island edge to the upper layer, because the

transition leads to a decrease in the contact area between the substrate and a new layer (Arciprete et al., 2006). As such atomic transitions to the upper layers lead to the strain field relaxation. The tradeoff between the cost of additional surface energy and the gain of energy due to elastic relaxation is the very driving force for the transition from 2D cluster to 3D islands (Kern and Muller, 1997; Chaparro et al., 2000). These arguments provide reason enough to consider situations when the atom hop probability to an upper layer can be higher than that to a lower layer. The kinetics of such a process could be described by adjusting the probability for atoms to hop up or hop down, which could subsequently lead to 2D cluster or 3D islands self-assembly (Arciprete et al., 2006).

While some simple computational approaches for 2D to 3D self-assembly were discussed before (i.e., (Brunev et al., 2001)), no complete 3D QD self-assembly model has been developed in which the growth from 2D cluster to 3D islands and the corresponding island size equalization can be clearly illustrated during the growth process. In this work we develop a fast multiscale 3D kinetic Monte Carlo (KMC) QD growth model. It is developed from our original (x,y) -plane growth model (Pan et al., 2004; Pan et al., 2006) by a fast algorithm for the long-range strain energy calculation and by introducing the up/down ratio for lateral self-organization (Pan et al., 2007).

With the proposed program, we have successfully simulated the transition of the 2D cluster to 3D island process. Furthermore, depositions with different flux rates are studied to show how the flux rate affects the island equalization during the deposition process.

Our model has also shown clearly the importance of the interruption time during the growth of QD islands. For the sake of extending these models to applications requiring strict control on the ordering, we also investigate the feasibility of using interrupted growth to create desired patterns on surfaces. This obviates the prevailing practice of hand-machining substrate morphology or seeding the surface through an extra step to encourage growth at specified locations. We believe that this model will provide an attractive means for producing predictably ordered nanostructures.

MODEL DESCRIPTION

The 3D layer-by-layer KMC growth model is developed from our 2D (x,y) -plane growth model (Pan et al., 2004; Pan et al., 2006). As in our previous model, the important contribution from the long-range elastic strain energy is included using a fast algorithm based on the Green's function method (Pan, 2002). Furthermore, to account for the out-of-plane (up and down) movement of the atoms, which is also called desorption and adsorption

(Lam and Vlachos, 2001; Lung et al., 2005), an up/down ratio is introduced.

First, the 2D hopping probability of an atom from one lattice site to a nearest or next nearest neighbor site in the (x,y) -plane is still governed by the Arrhenius law enhanced by the long-range strain energy field (Pan et al., 2004; Pan et al., 2006; Nurminen et al., 2001; Larsson, 2001). The Arrhenius law governing the hopping probability is given by

$$p = \nu_0 \exp\left(-\frac{E_s + E_n - E_{\text{str}}(x, y)}{k_B T}\right) \quad (1)$$

where ν_0 is the attempt frequency ($=10^{13}\text{s}^{-1}$), T the temperature, and k_B the Boltzmann's constant. Also in equation (1), E_s and E_n are the binding energies to the surface and to the neighboring atoms, respectively. Finally, $E_{\text{str}}(x,y)$, as a function of the plane coordinates (x,y) , is the energy correction from the long-range strain field due to the lattice mismatch between the substrate and the deposited material. As this long-range strain energy needs to be calculated repeatedly during the simulation, we have developed a fast algorithm by pre-calculating the energy along a unit circle and interpolating the energy at any location afterwards (Pan et al., 2007; Pan and Yang, 2003).

We calculate the binding energy to the neighboring atoms in the (x,y) -plane, E_n , using the following algorithm: We assume that the strength of a single nearest neighbor bond is E_b ($=0.3\text{eV}$), and it is reduced by a factor of α ($=1/\sqrt{2}$) for the next nearest neighbors. To evaluate the diffusion barrier, the binding energy at the site P_0 , where the diffusing atom is located, is calculated to be

$$E_{P_0} = nE_b + \alpha mE_b \quad (2)$$

with $n \leq 4$ and $m \leq 4$ being, respectively, the number of nearest and next nearest atoms. Similarly, for the site P_1 where the atom is going to hop to, we have

$$E_{P_1} = g(n'E_b + \alpha m'E_b) \quad (3)$$

where $n' \leq 4$ and $m' \leq 4$ are, respectively, the number of nearest and next nearest atoms at the new site P_1 , and g ($=0.2$) describes the coupling between the adjacent lattice sites (Meixner et al., 2003). Therefore, the overall binding energy E_n caused by neighbor interactions for an atom to jump from site P_0 to site P_1 is given by the difference of the binding energies at the corresponding lattice sites

$$E_n = (n - g \cdot n')E_b + (m - g \cdot m')\alpha E_b \quad (4)$$

Second, the binding energy to the surface of the (x,y) -plane, i.e. E_s , is assumed to be constant ($E_s=1.3\text{eV}$) in our previous 2D (x,y) -plane self-assembly model (Pan et al., 2004; Pan et al., 2006). However, in the 3D case (figure 1), the binding energy to the surface depends on the surface geometry of both the initial and final positions of the atoms. Based on recent molecular dynamics (MD)

calculation (Montalenti and Voter, 2001) and KMC simulation experience (Pan et al., 2004; Pan et al., 2006; Meixner et al., 2003) in 2D, we therefore propose the following simple equation for the 3D surface binding energy calculation.

$$E_s = (1-g)E_{s0} + (p-g \cdot p')\alpha E_{s0} + (q-g \cdot q')\alpha \cdot \alpha E_{s0} \quad (5)$$

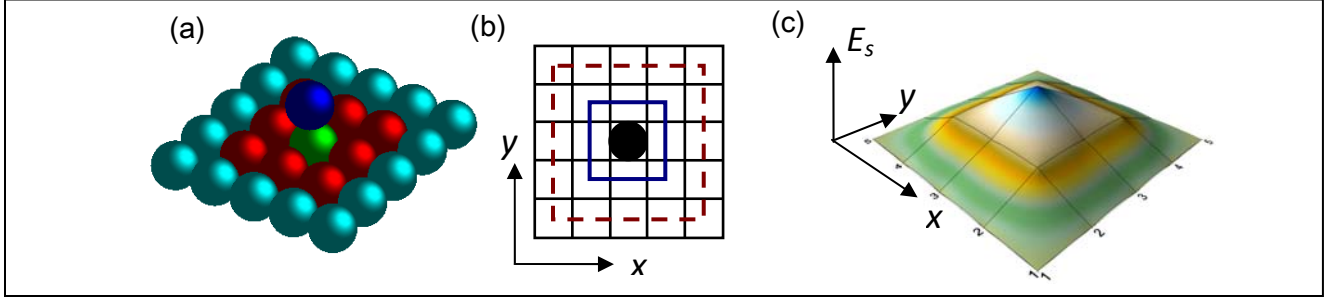


Figure 1 Schematic illustration of 3D QD self-assembly model. An atom on top of the substrate surface (x,y) -plane in (a), the relative locations of the atom grid on the (x,y) -plane in (b), the corresponding binding energy E_s related to the in-plane locations in (c).

where E_{s0} is the binding energy for the atom exactly under the selected adatom (figure 1), p, q are number of nearest and next nearest atoms in original position ($n' \leq 4, m' \leq 4$), p', q' are the number of nearest and next nearest atoms in the new position ($n' \leq 4, m' \leq 4$). The other two parameters, g and α , are used to scale the energy contribution from the atoms in the first and second squares (figure 1a, 1b). Assuming that the maximum surface binding energy to be 1.3eV as before for the 2D growth simulation (Pan et al., 2004; Pan et al., 2006) which means that all the positions under this adatom are occupied by atoms, we can find $E_{s0}=0.28\text{eV}$ from equation (5) by back-calculation.

Finally, as discussed in the introduction, the growth system always tries to decrease its free energy by moving atoms at the edge to upper layer to form 3D islands. The possibility for an atom to hop to a higher or lower layer depends on the material properties and growth conditions (Arciprete et al., 2006). To account for the up and down jump activities of the atoms, the parameter up/down ratio ρ is introduced, which is defined as the ratio of the possibility for edge atoms hopping up to that hopping down. In other words, if we let P_{up} be the jump up possibility and P_{down} the jump down possibility, then the up/down ratio $\rho = P_{\text{up}}/P_{\text{down}}$. It is further remarked that the up/down ratio actually reflects the balance between surface energy increase and strain energy decrease. This physical activity is illustrated in figure 2 where layer 1 is the substrate and the atom “A” is on the edge of layer 2 of the deposited atoms (i.e., within the QD island). It is also understandable that the up or down jump possibility of atom “A” is controlled only by the up/down ratio instead of by the individual jump up and down possibilities. Moreover, strictly speaking, since the strain energy changes along the island height direction, the up/down ratio is, in general, not constant in different island layers.

However, in order to extract the important contribution of the up/down ratio, we assume that the up/down ratio is constant. In other words, it is only affected by the geometry around it but not by the layer position. Furthermore, in order to form 3D islands, the number of atoms jumping up should be larger than those jumping down, which means that ρ should be larger than 1. Otherwise, all the atoms will tend to move to lower layer to form the layer-by-layer Frank-van der Merwe structure.

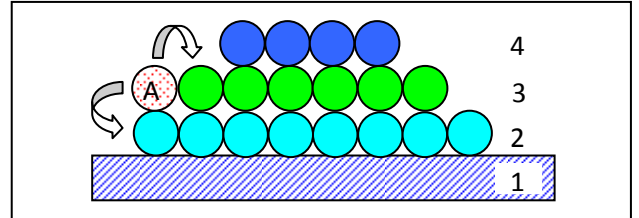


Figure 2. Illustration of the up or down jump for an edge atom A during 3D QD self-assembly.

RESULTS: PARAMETER STUDIES OF ρ

Using the 3D QD self-assembly approach described above, we can now simulate the epitaxial growth process. The growth model contains 100×100 grids with periodic boundary conditions, and the material is InAs/GaAs (001). We first study the effect of variations in ρ on the island height. The validation of recognizable pattern formations was performed extensively with independent results in the literature in (Pan et al., 2007) and (Zhu et al., 2007). Shown in figure 3 are the islands distributions. It is observed clearly from figure 3 that 1) the average island height increases with increasing ρ (for small ρ , say, $\rho \leq 5$, basically only 2D growth is observed); 2) island size and shape are very sensitive ρ when it is less than 20; 3) it is worthy to remark that ρ determines the 2D to 3D

transition instead of the absolute value of P_{up} and P_{down} . This ratio is directly proportional to the ratio of the ascending (desorption) and descending (adsorption) atoms on the surface (Lam and Vlachos, 2001; Russo and Smereka, 2006).

To further understand the effect of variations in ρ on the average island height the data in figure 3 are analyzed along with more simulated results for large up/down ratios. The relation between the average island height and ρ is presented in figure 4. Figure 4 demonstrates that 1) the average island height experiences sharp changes when ρ varies from 3 to around 20. The island height increases with increasing ρ ; 2) when ρ is larger than 20, the curve asymptotically approaches a maximal island height of approximately 20 grid spacings. This means that the average island height will mostly keep at a constant maximum value when the up/down ratio is large (say, $\rho > 30$); 3) an identifiable inflection point, approximately at $\rho = 13$, physically corresponds to the critical transition point from 2D cluster growth to 3D islands growth. This up/down ratio is roughly equivalent to the surface and bulk energy ratio as was demonstrated in (Brunev et al., 2001; Kratzer et al., 2006) using different approaches.

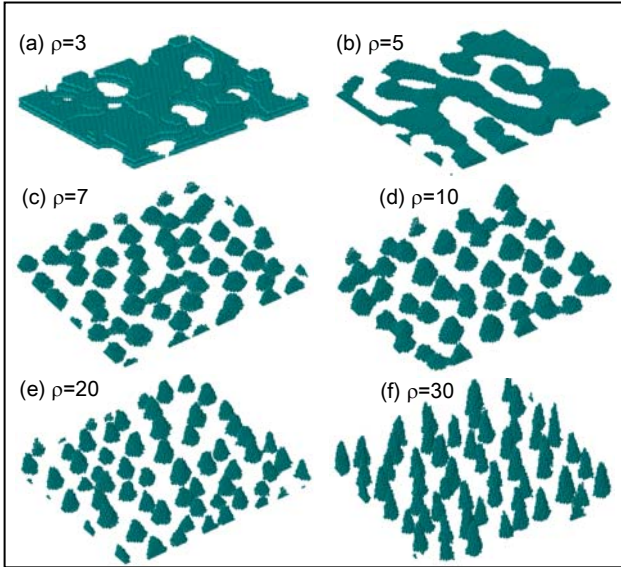


Figure 3 3D island distributions for different up/down ratios ρ with total coverage $c=1.6\text{ML}$. Fixed growth parameters are $T=700\text{K}$, $F=0.01\text{ML/s}$, and interruption time $t_i=200\text{s}$ (The total simulation time = the deposition time ($t_d=160\text{s}$) plus the interruption time ($t_i=200\text{s}$)).

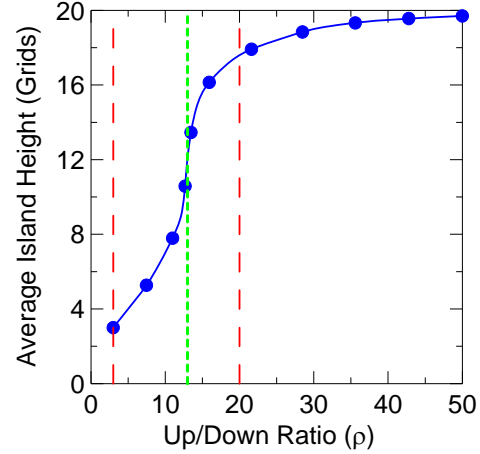


Figure 4. Average island height vs. ρ for $\rho=3$ to 50. Fixed growth parameters are $T=700\text{K}$, $F=0.01\text{ML/s}$, $c=1.6\text{ML}$, and interruption time $t_i=200\text{s}$.

RESULTS: ISLAND SIZE & DISTRIBUTION

Island size equalization relies on the movement of atoms on the surface during epitaxial growth. Equalization starts from the very beginning of the deposition process and reaches equilibrium with sufficient growth time (Pan et al., 2004). Figure 5 demonstrates the island size dependence on growth times for three different up/down ratios ($\rho=10, 20$, and 30 in the first, second, and third row). Island distributions immediately after the deposition (i.e., the interruption time $t_i=0$) are shown in the first column, 100 seconds after the deposition ($t_i=100\text{s}$) in the second column, and 200 seconds after deposition ($t_i=200\text{s}$) in the third column (figure 5). It is observed from figure 5 that: 1) for a fixed up/down ratio ($\rho=10, 20$, and 30), with increasing interruption time, small isolated islands assemble to form large ones, and the island distribution becomes increasingly ordered; 2) for fixed interruption time ($t_i=0, 100\text{s}$, and 200s), an increasing up/down ratio, in general, increases the height of the islands (changes the shape of the islands), similarly observed in figure 3. Since ρ is closely related to the surface and bulk energy ratio, this may enable experimentalists with additional control to optimize the island shape and distribution.

While figure 5 illustrates the influence of the interruption time on the island size, figures 6 and 7 demonstrate further the effect of the deposition time on the island shape and size for fixed up/down ratio $\rho=10$. In figure 6, island size equalization starts from the beginning of the deposition process and becomes larger with increasing deposition ($t_d=50\text{s}, 100\text{s}, 160\text{s}$) and interruption time ($t_i=200\text{s}$). Furthermore, with increasing island size, the number of islands decreases. This relation can be observed from the histogram in figure 7 for the relationship between the island diameter (of the

equivalent circle at the bottom of the island) and the corresponding number of islands.

Figure 8 shows the effect of the flux rate ($F=1\text{ML/s}$, 0.1ML/s and 0.01ML/s) on the island distribution. For a low flux rate (e.g. at $F=0.01\text{ML/s}$), the atoms are afforded more time to move to the equilibrium position during the deposition process and to assemble together. A low flux rate (say, $F=0.01\text{ML/s}$) usually corresponds to larger and more ordered islands.

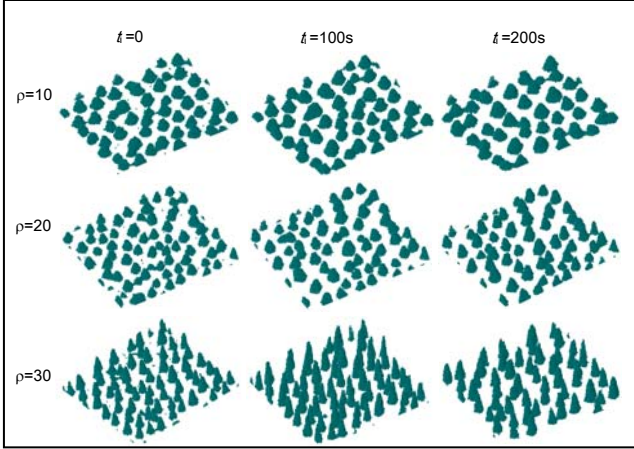


Figure 5. Island distributions for different interruption times ($t_i=0\text{s}$, corresponding to deposition time $t_d=160\text{s}$, $t_i=100\text{s}$, and $t_i=200\text{s}$) and for different up/down ratios ($\rho=10$, 20 and 30). Fixed growth parameters are $T=700\text{K}$, $F=0.01\text{ML/s}$, and $c=1.6\text{ML}$.

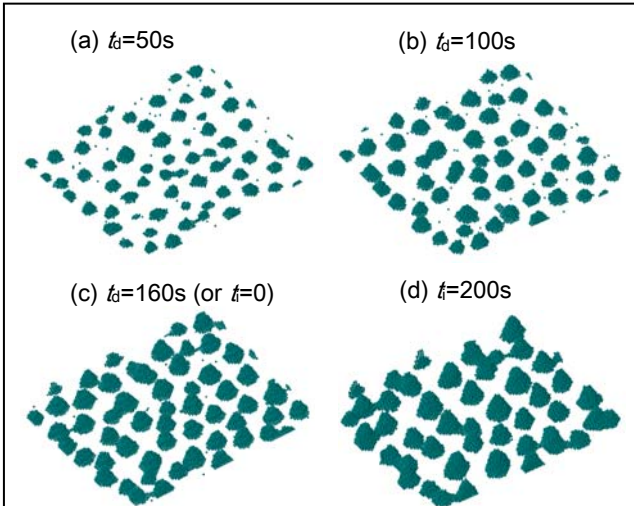


Figure 6. Island distributions during and after deposition. Deposition time $t_d=50\text{s}$ with 0.5ML coverage in (a), $t_d=100\text{s}$ with 1ML coverage in (b), $t_d=160\text{s}$ with coverage 1.6ML in (c) and interruption time $t_i=200\text{s}$ in (d). $T=700\text{K}$, $F=0.01\text{ML/s}$, $c=1.6\text{ML}$, and $\rho=10$.

RESULTS: PREPATTERNING

Control of pattern formations is currently enabled through premachining of the substrate with pore arrays

(Atkinson et al., 2006) or masked substrates (Liang et al., 2004), both of which require substantial increase in total fabrication time. A nominal change to the interruption time, however, reveals that pattern quality (i.e. larger size and repeated ordering of dots) can be obtained (Pan et al., 2007). In figure 9, significant differences in pattern quality can be observed between traditional continuous deposition (figure 9a) versus employing a growth pause for 50 seconds after an initial 0.3ML deposit and interruption at 150 seconds after 1.6ML deposit.

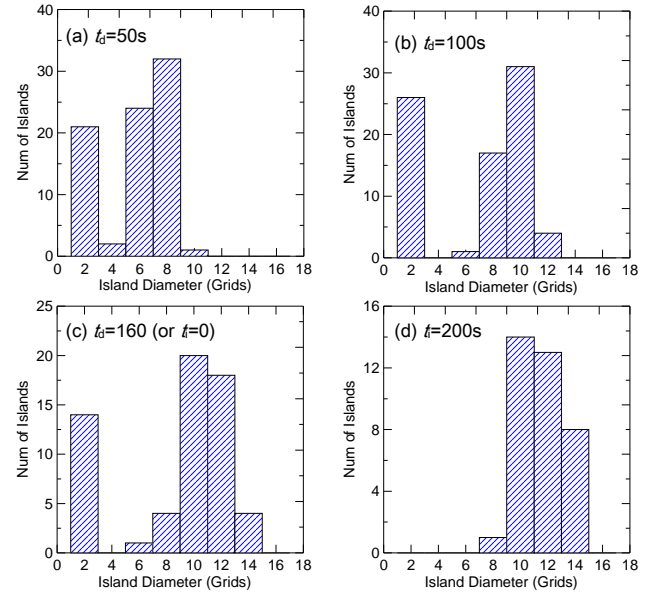


Figure 7. Average island diameter (of the bottom equivalent circle of the island) vs. number of islands during and after deposition. $T=700\text{K}$, $F=0.01\text{ML/s}$, $c=1.6\text{ML}$ and $\rho=10$.

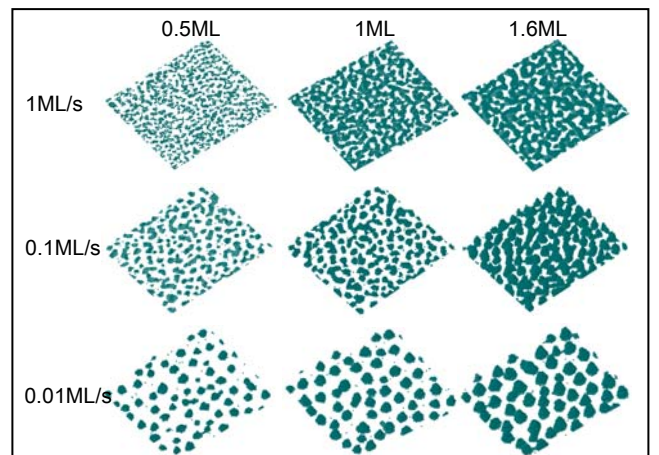


Figure 8. Island distributions for different deposition processes of 0.5ML , 1ML and 1.6ML with flux rates $F=1\text{ML/s}$, 0.1ML/s and 0.01ML/s . Fixed growth parameters are $T=700\text{K}$, $c=1.6\text{ML}$ and $\rho=10$.

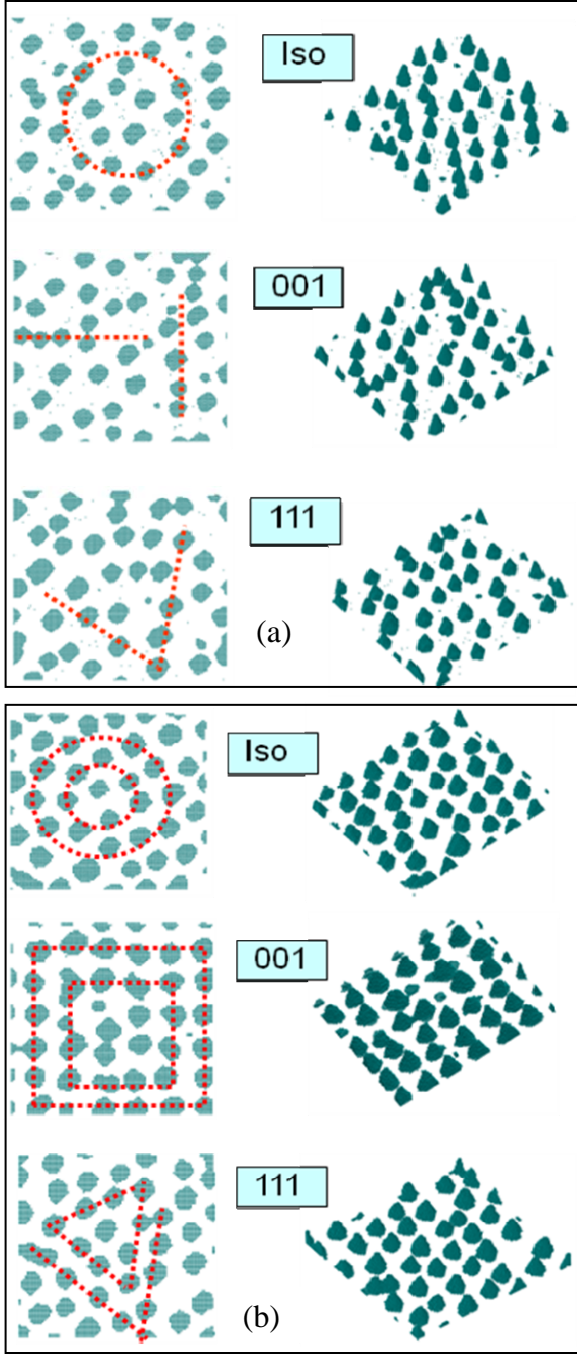


Figure 9. Comparison of (a) continuous growth and (b) prepatterned growth using variations of substrate symmetries (isotropic, (001), and (111)) at $T=700\text{K}$, coverage of 1.6ML and $\rho=10$.

RESULTS: CORRELATED GROWTH

Finally, using the fundamental developments from (Pan, 2002) that are used in the 3D KMC model, the effect of the buried height of nanostructures on correlated growth in superlattices is investigated. It has been shown that the depth to which QDs are buried in layered structures influences patterns on subsequently grown layers (Holý et al., 1999; Wang et al., 2004). The mechanism that enables this is the interaction of mechanical strain fields owing to the embedding strain of the array of QDs. In particular, Wang et al. showed the strain driven correlation and anticorrelation of InGaAs QDs in detail through cross-sectional STM images.

Using the Green's Functions developed in (Pan, 2002), we computed the strain energy values on the surface due to a buried structure in an elastic half-space. The degree of burial is varied to modulate the degree of strain interaction between the buried QDs and the surface. The dark regions in Figure 10 show regions of increased strain energy where the higher accompanying strain implies that coherent structures like QDs are more likely to grow. This is due to the local relaxation of the degree of lattice mismatch at those regions where the strain fields interact constructively. It is noteworthy that for $D=2$ the (001) growth is correlated, which agrees convincingly with those of the STM images in (Wang et al., 2004) at small burial heights. At $D=20$ the (001) growth is anti-correlated which also corresponds to the anti-correlation achieved with increased burial depth in (Wang, et al., 2004).

It is furthermore noteworthy that from the calculations, we show that the (111) growths do not exhibit anti-correlation by increasing the burial depth to $D=20$ in contrast with the observations from the (001) case. In fact, the growth remains strictly correlated. Although the (111) growth correlation remains to be shown experimentally, the absence of anti-correlation at deeper burial depths appears to be caused by the lack of strain field interactions at the anti-correlated sites due to the additional effect of anisotropy and the overall change in symmetry caused by the change in growth direction.

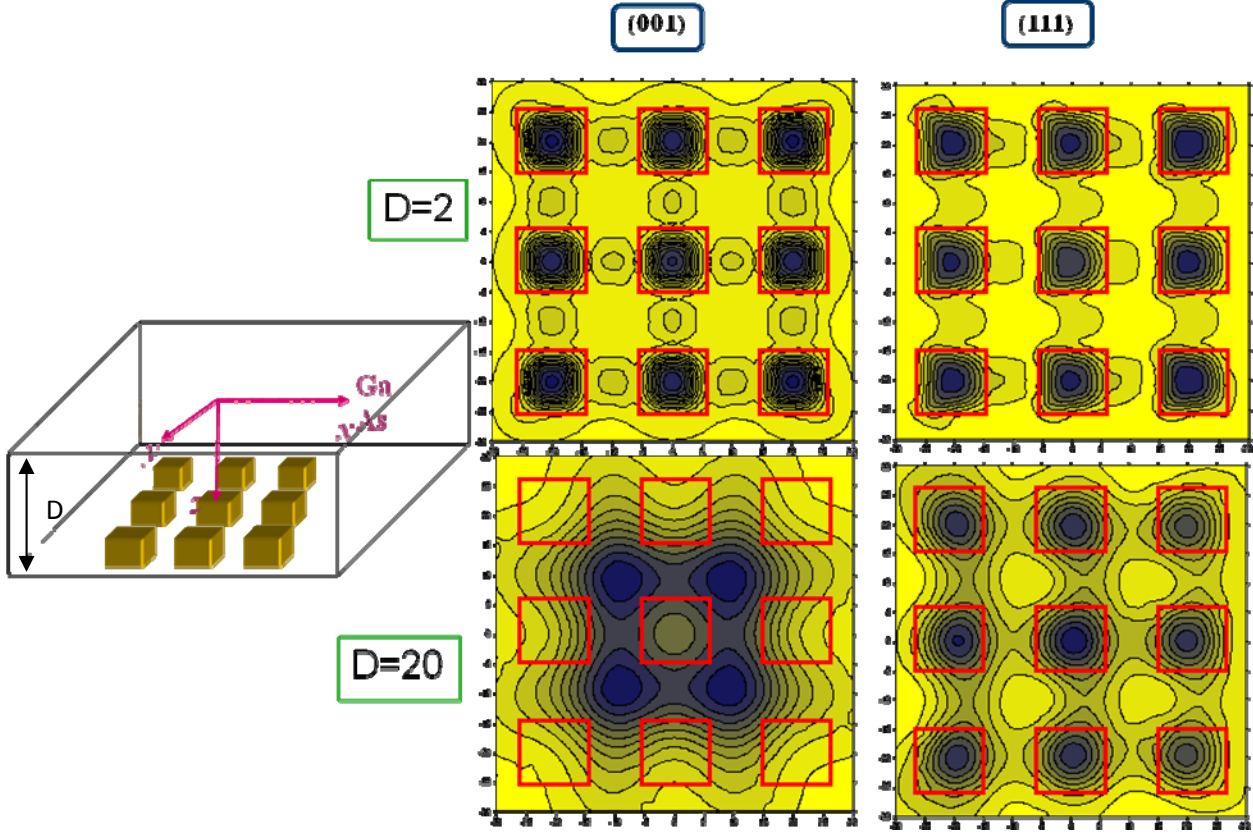


Figure 10. Strain energy contours of 3x3 buried array at two different depths and two different growth directions. Dark areas indicate regions of favorable growth for the next layer.

CONCLUSIONS

In this report, we propose a 3D QD epitaxial growth model by enhancing our former (x,y)-plane growth model with a fast algorithm for long-range strain energy calculation and an up/down jump ratio for the diffusion atoms. Specifically, the balance between surface energy increase and bulk energy decrease is demonstrated by introducing the up/down ratio. Further studied is the dependence of the island height and shape on the up/down ratio. Combining the up/down ratio and one of the growth parameters (i.e., flux rate), island equalization during deposition process and after deposition is demonstrated.

The developments have also enabled three new fundamental results. The first is the consistent validation of pattern formations for general quantum dot growth on surfaces. By considering only the chemical species used in the material fabrication, fabrication parameters such as temperature and flow rate, and the symmetry of the substrate surface plane, we can repeatedly reproduce the patterns obtained from numerous independent results from the literature. Based only on the experimental parameters reported in those papers, the new modeling theory accurately reproduces the quantum dot arrangements.

The second result is a new fabrication procedure that obviates tooling for prepatterned growth when strict control is required on the first surface grown directly on the substrate layer. By adjusting species flow rates during growth, we have simulated a technique for controlling the pattern quality on surfaces. Whereas earlier efforts attempted to seed growth by mechanically creating “dimples” on the substrate, the new method enables ripening to coalesce smaller dots into larger ones, thereby producing more pronounced dot sizes in specifiable patterns without machining the substrate.

The third result is the development of a through-thickness dot correlation technique for superlattices where elastic fields generated from buried quantum dots are demonstrated to provide another means of controlling surface pattern quality. Dots among different layers can interact and produce correlated and anticorrelated patterns. Although the capping layer thickness has been known to produce this effect, these simulated results are the first of its kind.

ACKNOWLEDGEMENTS

The authors gratefully acknowledge support from the Defense Threat Reduction Agency Joint Science and Technology Office (DTRA-JSTO) and computing resources from the ARL Major Shared Resource Center.

REFERENCES

- Arciprete, F., Placidi, E., Sessi, V., Fanfoni, M., Patella, F., Balzarotti, A., 2006. *Appl. Phys. Lett.* 89, 041904.
- Atkinson, P., Bremner, S. P., Anderson, D., Jones, G. A. C., Ritchie, D. A., 2006. *J. Vac. Sci. Technol. B*, 24(3), 1523.
- Bimberg, D., Grundmann, M., Ledentsov, N. N., 1998. *Quantum Dot Heterostructures*, Wiley, Chichester.
- Bressler-Hill, V., Varma, S., Lorke, A., Noshov, B. Z., Petroff, P. M., Weinberg, W. H., 1995. *Phys. Rev. Lett.* 74, 3209-3212.
- Brunev, D. V., Neizvestny, I. G., Shwartz, N. L., Yanovitskaja, Z. S., 2001. *Nanotechnology* 12, 413-416.
- Chaparro, S. A., Zhang, Y., Drucker, J., Chandrasekhar, D., Smith, D. J., 2000. *J. Appl. Phys.* 87 2245-2254.
- Holý, V., Springholz, G., Pinczolit, M., Bauer, G. 1999, *Phys. Rev. Lett.*, 83, 356.
- Joyce, B. A., Vvedensky, D. D., 2004. *Mater. Sci. Eng.*, R. 46, 127-176 (2004).
- Kern, R., Muller, P., 1997. *Surf. Sci.* 392, 103-133
- Kratzer, P., Liu, Q. K. K., Acosta-Diaz, P., Manzano, C., Costantini, G., Songmuang, R., Rastelli, A., Schmidt, O. G., Kern, K., 2006. *Phys. Rev. B* 73, 205347.
- Lam, R., Vlachos, D. G., 2001. *Phys. Rev. B* 64, 035401.
- Larsson, M., 2001. *Phys. Rev. B* 64, 115428.
- Liang, J., Luo, H., Beresford, R., Xu, J., 2004. *Appl. Phys. Lett.*, 85, 5974.
- Lung, M. T., Lam, C. H., Sander, L. M., 2005. *Phys. Rev. Lett.* 95, 086102.
- Meixner, M., Kunert, R., Schöll, E., 2003. *Phys. Rev. B* 67, 195301.
- Montalenti, F., Voter, A. F., 2001. *Phys. Rev. B* 64, 081401.
- Musikhin, Yu. G., Cirilin, G. E., Dubrovskii, V. G., Samsonenko, Yu. B., Tonkikh, A. A., Bert, N. A., Ustinov, V. M., 2005. *Semiconductors*. 39, 820-825.
- Nurminen, L., Kuronen, A., Kaski, K., 2001. *Phys. Rev. B* 63, 035407.
- Pan, E., 2002. *J. Appl. Phys.* 91, 6379-6387.
- Pan, E., Sun, M., Chung, P. W., Zhu, R., 2007. *Appl. Phys. Lett.*, 91, 193110.
- Pan, E., Yang, B., 2003. *Appl. Math. Model.* 27, 307-326.
- Pan, E., Zhu, R., Chung, P. W., 2004. *J. Nanoeng. Nanosys.* 218, 71-82.
- Pan, E., Zhu, R., Chung, P. W., 2006. *J. Appl. Phys.* 100, 013527.
- Pao, C. W., Srolovitz, D. J., 2006. *J. Mech. Phys. Solids* 54, 2527-2543.
- Pcheljakov, O. P., Markov, V. A., Nikiforov, A. I., Sokolov, L. V., 1997. *Thin Solid Films* 306- 310, 299 (1997).
- Russo, G., Smereka, P., 2006. *J. Comput. Phys.* 214, 809-828.
- Sage, J. F., Barvosa-Carter, W., Aziz, M. J., 2000. *Appl. Phys. Lett.* 77, 516-518.
- Shchukin, V. A., Bimberg, D., 1999. *Rev. Mod. Phys.* 71, 1125-1171 (1999).
- Stangl, J., Holy, V., Bauer, G., 2004. *Rev. Mod. Phys.* 76, 725-783.
- Sun, Y., Miyasato, T., Wigmore, J. K., 2000. *J. Appl. Phys.* 87, 8483-8486.
- Wang, X. D., Liu, N., Shih, C. K., Govindaraju, S., Holmes, Jr, A. L. 2004, *Appl. Phys. Lett.*, 85, 1356.
- Zandvliet, H. J. W., Poelsema, B., 1999. *Phys. Rev. B* 59, 7289-7292.
- Zhu, R., Pan, E., Chung, P. W., 2007, *Phys. Rev. B.*, 75, 205339.
- Zoethout, E., Guerlue, O., Zandvliet, H. J. W., Poelsema, B., 2000. *Surf. Sci.* 452, 247-252.